

Article

The Design of an Anti-Synchronization Control Algorithm for a 4D Laser System

Zuoxun Wang ^{1,2,*}, Jinhao Pan ^{2,*}, Lei Ma ¹ and Guijuan Wang ^{3,*}

¹ School of Mechanical and Electrical Engineering, Shandong Xiehe University, Jinan 250107, China; malei@sdxiehe.edu.cn

² School of Information and Automation, Qilu University of Technology (Shandong Academy of Sciences), Jinan 250353, China

³ School of Information and Electrical Engineering, Shandong Jianzhu University, Jinan 250101, China

* Correspondence: wangzuoxun@qlu.edu.cn (Z.W.); 201802120027@stu.qlu.edu.cn (J.P.); wgj_wzx@sdjzu.edu.cn (G.W.)

Abstract: When studying the control problems of nonlinear systems, there are always uncertainties and disturbances. The existence of this phenomenon will increase the error in production engineering and reduce work efficiency. In order to reduce the nonlinear asymmetric control, the control method of a laser hyperchaotic system is designed in this paper. The system is a complex number system, with remarkable nonlinear characteristics. The system is divided into two parts by calculating the state transformation matrix, which shows that the system can realize simultaneous synchronization and anti-synchronization. Firstly, in the ideal case, the stabilization, synchronization, and anti-synchronization of the system are studied by using the dynamic gain feedback method, and a dynamic feedback controller is designed. Secondly, in the case of uncertainty and disturbance, a dynamic feedback control strategy based on uncertainty and disturbance estimator (UDE) is proposed. With the aim to solve the control problem of the system, the corresponding controller is designed to modify the system. Finally, through simulation and comparison, it is verified that the effect of this method is remarkable.



Citation: Wang, Z.; Pan, J.; Ma, L.; Wang, G. The Design of an Anti-Synchronization Control Algorithm for a 4D Laser System. *Symmetry* **2022**, *14*, 710. <https://doi.org/10.3390/sym14040710>

Academic Editor: Christos Volos

Received: 5 March 2022

Accepted: 24 March 2022

Published: 31 March 2022

Publisher's Note: MDPI stays neutral with regard to jurisdictional claims in published maps and institutional affiliations.



Copyright: © 2022 by the authors. Licensee MDPI, Basel, Switzerland. This article is an open access article distributed under the terms and conditions of the Creative Commons Attribution (CC BY) license (<https://creativecommons.org/licenses/by/4.0/>).

Keywords: nonlinear; stabilization; synchronization; anti-synchronization; dynamic feedback control; UDE

1. Introduction

Nonlinearity is a common phenomenon in nature, such as laser generation, subharmonic oscillation, self-excited oscillation, frequency capture, the development of human society, people's thinking process, etc. [1–4]. These are nonlinear changes with time. With the development of science and technology, nonlinear problems appear in many disciplines. Chaos is a very important aspect of nonlinear dynamics. It is of great significance in the study of various problems.

In nature and human society, synchronization and anti-synchronization refer to the coordination between the phases of at least two vibration systems or the opposite trajectory (or beat). This is a natural phenomenon in nonlinear systems. In the hyperchaotic system studied in this paper, there are simultaneous synchronization and anti-synchronization phenomena. In the realization of chaos control, making full use of the characteristics of chaos is very important for determining the control target and selecting the control method [4]. In modern industrial production, mobile robots and UAVs can be described using nonlinear systems. There are always uncertainties and external disturbances in the system. These problems will lead to the asymmetry of the system. In practical problems, the movement of multiple robots cannot be coordinated, and the industrial production efficiency is low. In order to reduce the asymmetric control problem in nonlinear systems, a dynamic control method based on uncertainty and disturbance is proposed in this

paper. The essence of UDE is to establish an interference estimator to estimate unknown interference variables. Based on the UDE control method and dynamic gain control method, the stabilization, synchronization, and anti-synchronization of hyperchaotic systems are studied in this paper.

Chaos has its applications in many fields. With the rapid development of modern communication technology, optical chaos and its secure communication technology have received extensive attention from researchers because of their unique advantages. The introduction of additional degrees of freedom into semiconductor lasers can produce rich nonlinear dynamic behavior [5,6]. If appropriate control parameters are selected, high-dimensional chaotic optical signals can be output. A chaotic optical signal is especially suitable for chaotic secure communication [7–10]. In addition, in 2001, Nakamura et al. first proposed chaotic paths and applied them to mobile robots to achieve full coverage of the area [11]. This has led to the application of chaos in the field of robotics. For different occasions, Chaos mobile robots can work with different sensors to meet different needs [12–14].

In this paper, the dynamic feedback control method based on UDE is applied to plural systems. The 4D laser system has two positive Lyapunov functions and is hyperchaotic. The system is more complex than the real number system, and the nonlinear characteristics are more obvious. Therefore, the study of this system can well verify the effectiveness of this method, and the research problems of this system can provide a theoretical basis for the study of chaotic mobile robots. The simultaneous synchronization and anti-synchronization [15] of a system mean that some states of a system can be synchronized, while other states can be anti-synchronized under the action of an appropriate controller. The study of this problem provides a theoretical basis for the subsequent implementation of multiple chaotic mobile robots to achieve difficult maneuvers. It enables multiple robots to achieve the same or opposite actions simultaneously. The study of the stabilization problem can improve the coverage and stability of chaotic mobile robots in path planning. By studying the control problem of nonlinear systems, the asymmetric control phenomenon of the system is reduced, and the stability of nonlinear systems is improved.

2. Preliminary

Lemma 1. Consider the following system:

$$\dot{z} = f(z) + bu \quad (1)$$

where $z \in R^n$ is the state vector, $f(z) \in R^n$ is vector function, $b \in R^{n \times r}$ is the constant matrix, and $r \geq 1$, $u \in R^r$ is the controller to be designed. According to results in Refs. [2,16], if $(f(z), b)$ is stabilizable, then the designed dynamic gain feedback controller [16,17] is

$$u = kz \quad (2)$$

where $k = k(t)b^T$, and feedback gain $k(t)$ update law is as follows:

$$\dot{k}(t) = -\|z(t)\|^2 \quad (3)$$

Lemma 2. A chaotic system with model uncertainty and external disturbance can be expressed as

$$\dot{z} = f(z) + bu_d + Bu \quad (4)$$

$$u_d = \Delta f(z) + d(t) \quad (5)$$

where z is the state, $\Delta f(z)$ is model uncertainty, and $d(t)$ is an external disturbance. u_d meets the following structural constraints:

$$[I - BB^+]u_d \equiv 0 \quad (6)$$

where I is an n -order identity matrix; $B^+ = (B^T B)^{-1} B^T$.

The filter $g(t)$ to be designed needs to satisfy the following conditions:

$$\tilde{u} = \hat{u}_d - u_d \rightarrow 0, t \rightarrow \infty \tag{7}$$

where $\hat{u}_d = (\dot{z} - f(z) - Bu_{ude}) * g_f(t)$, and \hat{u}_d is u_d estimate.

Therefore, it can be obtained that the controller u to be designed is [15,18]: $u = u_a + u_{ude}$, where u_a is a controller designed by using the dynamic gain control method.

$$u_a = k(t)B^T z(t) \tag{8}$$

$$u_{ude} = b \left\{ -\ell^{-1} \left[\frac{sG(s)}{1 - G(s)} \right] * z(t) + \ell^{-1} \left[\frac{G(s)}{1 - G(s)} \right] * F(z) \right\} \tag{9}$$

where $G(s) = \ell[g(t)]$, ℓ^{-1} is inverse Laplace transform, $*$ is convolution, and $k(t) = -\|z(t)\|^2$.

Definition 1. For the Lorenz system (10) and its slave system (11),

$$x = h(x) = \begin{pmatrix} a(x_2 - x_1) \\ bx_1 - x_2 - x_1x_3 \\ cx_3 + x_1x_2 \end{pmatrix} \tag{10}$$

$$q = h(q) + BU \tag{11}$$

If variables x_1, x_2 of the system (10) are anti-synchronous with two variables q_1, q_2 of another system (11), at the same time, x_3 is synchronous with q_3 , the master system (10) and the slave system (11) realize simultaneous synchronization and anti-synchronization.

3. Problem Formulation

In this paper, a multi-winged butterfly laser complex chaotic system is studied. The model of a 4D laser hyperchaotic system is as follows:

$$\begin{cases} \dot{x}_1 = -f_1x_1 + x_1x_2 + x_3x_4 + f_0[1 + \sin(\Omega t)] \\ \dot{x}_2 = -f_2x_2 - 0.5(x_1^2 - x_3^2) \\ \dot{x}_3 = -f_1x_3 + x_1x_4 - x_2x_3 \\ \dot{x}_4 = -f_2x_4 - x_1x_3 \end{cases} \tag{12}$$

where $x_{1,2,3} \in C, x_4 \in R$. When $f_0 = f_1 = f_2 = 0.01, \Omega > 0.22$ or $0.45 < \Omega < 0.98$, system (12) has two positive Lyapunov functions, which are hyperchaotic. System (12) first appeared in [19]. Based on this model, the stabilization problem and simultaneous synchronization and anti-synchronization problems are studied in this paper.

Let $x_1 = z_1 + jz_2, x_2 = z_3 + jz_4, x_3 = z_5 + jz_6, x_4 = z_7, j = \sqrt{-1}$; through the transformation, the complex system is transformed into a 7D real system, as shown below.

$$\dot{z} = f(z) \tag{13}$$

$$f(z) = \begin{pmatrix} -f_1z_1 + z_2z_3 + z_5z_7 + f_0[1 + \sin(\Omega t)] \\ -f_1z_2 + z_2z_4 + z_6z_7 \\ -f_2z_3 - 0.5(z_1^2 - z_5^2) \\ -f_2z_4 - 0.5(z_2^2 - z_6^2) \\ -f_1z_5 + z_1z_7 - z_3z_5 \\ -f_1z_6 + z_2z_7 - z_4z_6 \\ -f_2z_7 - z_1z_5 \end{pmatrix} \tag{14}$$

where $z \in R^7$ is the state vector; f_0 , f_1 and f_2 are given in Equation (10), and when $\Omega = 0.6$, the phase diagram of the system (14) has butterfly chaotic attractor. The vector field divergence of the system is

$$\nabla V = \frac{\partial \dot{z}_1}{z_1} + \frac{\partial \dot{z}_2}{z_2} + \frac{\partial \dot{z}_3}{z_3} + \frac{\partial \dot{z}_4}{z_4} + \frac{\partial \dot{z}_5}{z_5} + \frac{\partial \dot{z}_6}{z_6} + \frac{\partial \dot{z}_7}{z_7} = -4f_1 - 3f_2$$

When $\nabla V < 0$, the system is dissipative; as $\nabla V = -0.07 < 0$ in this paper, it satisfies the dissipative condition; the motion of the system (14) is eventually fixed to the attractor. The phase diagram of chaotic attractor was shown in Figure 1.

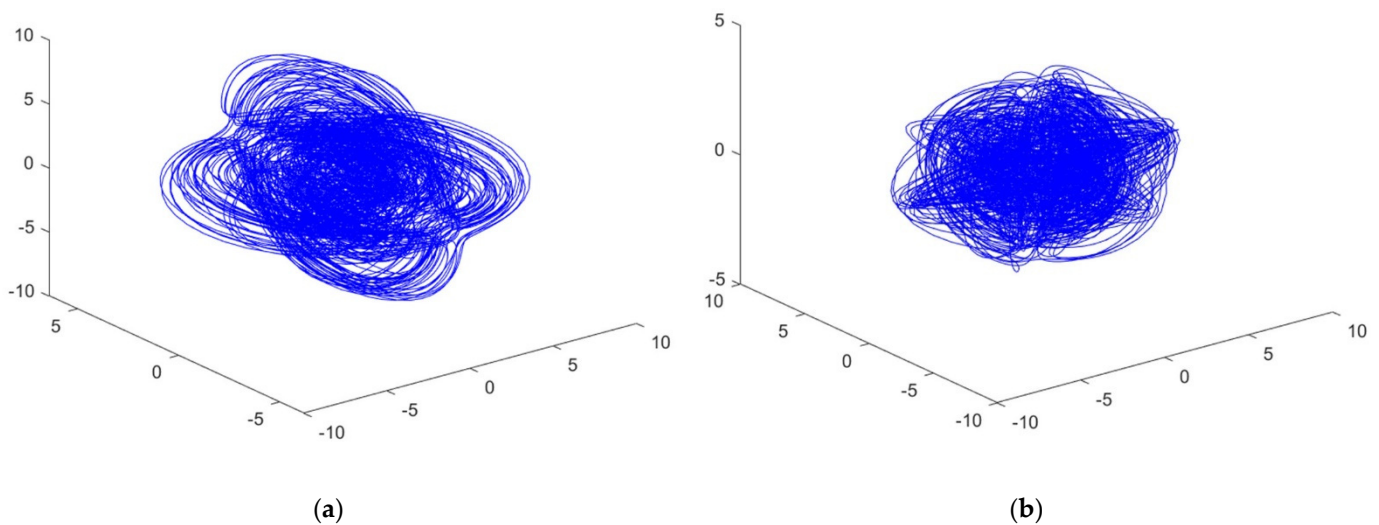


Figure 1. The phase diagram of chaotic attractor: (a) the phase diagram of z_1, z_3, z_5 ; (b) the phase diagram of z_1, z_5, z_7 .

In this paper, the suitable controllers are designed by using the control method of dynamic gain feedback. Then, this method is combined with the control method based on UDE to design more reasonable controllers.

4. Methods and Materials

4.1. Stabilization Problem

Before studying the simultaneous synchronization and anti-synchronization of the system, in this part, the stabilization of the system is first discussed. Firstly, the dynamic gain control method [20–22] was used to study the nominal system.

Theorem 1. First, the nominal system is as follows:

$$\dot{z} = f(z) + Bu_a \quad (15)$$

where z is the state vector, B is given as

$$B^T = \begin{pmatrix} 1 & 0 & 0 & 0 & 0 & 0 & 0 \\ 0 & 0 & 1 & 0 & 0 & 0 & 0 \\ 0 & 0 & 0 & 1 & 0 & 0 & 0 \\ 0 & 0 & 0 & 0 & 0 & 0 & 1 \end{pmatrix} \quad (16)$$

and u_a is the designed controller; u_a is presented as

$$u_a = K(t)B^T z(t) \quad (17)$$

where $K(t)$ the designed dynamic gain feedback, and it is updated by

$$\dot{K}(t) = -\|z(t)\|^2 \tag{18}$$

by which system (15) achieves stabilization.

Proof of Theorem 1. When $z_1 = z_3 = z_4 = z_7 = 0$, the following subsystem

$$\dot{z}_2 = -f_1 z_1 \tag{19}$$

$$\dot{z}_5 = -f_1 z_5 \tag{20}$$

$$\dot{z}_6 = -f_1 z_6 \tag{21}$$

is asymptotically stable; then, $(f(z), B)$ is stabilized. According to Lemma 1, the controller u_a is given in (17), which completes the proof. \square

The system can be expressed as follows:

$$\begin{aligned} \dot{z}_1 &= -f_1 z_1 + z_1 z_3 + z_5 z_7 + f_0 [1 + \sin(\Omega t)] + Kz_1 \\ \dot{z}_2 &= -f_1 z_2 + z_2 z_4 + z_6 z_7 \\ \dot{z}_3 &= -f_2 z_3 - 0.5(z_1^2 - z_5^2) + Kz_3 \\ \dot{z}_4 &= -f_2 z_4 - 0.5(z_2^2 - z_6^2) + Kz_4 \\ \dot{z}_5 &= -f_1 z_5 + z_1 z_7 - z_3 z_5 \\ \dot{z}_6 &= -f_1 z_6 + z_2 z_7 - z_4 z_6 \\ \dot{z}_7 &= -f_2 z_7 - z_1 z_5 + Kz_7 \end{aligned} \tag{22}$$

Next, the stabilization of the system (4) was studied.

Let $b^T = (0 \ 0 \ 0 \ 0 \ 0 \ 0 \ 1)$, that is, the disturbance is added to the state z_7 .

$$\Delta f(z) = \begin{pmatrix} 0 \\ 0 \\ 0 \\ 0 \\ 0 \\ 0 \\ 0.1z_1^2 \end{pmatrix}, d(t) = \begin{pmatrix} 0 \\ 0 \\ 0 \\ 0 \\ 0 \\ 0 \\ 2 \end{pmatrix} \tag{23}$$

According to Lemma 2, we can obtain u_{ude} , and filter selection is as follows [23,24]:

$$G(s) = \frac{10\omega_0 s + (a - \omega_0^2)}{s^2 + 10\omega_0 s + a} \tag{24}$$

where $\omega_0 = 4\pi$, $a = 100\omega_0^2$. The controlled chaotic system is

$$\begin{aligned} \dot{z}_1 &= -f_1 z_1 + z_1 z_3 + z_5 z_7 + f_0 [1 + \sin(\Omega t)] + Kz_1 \\ \dot{z}_2 &= -f_1 z_2 + z_2 z_4 + z_6 z_7 \\ \dot{z}_3 &= -f_2 z_3 - 0.5(z_1^2 - z_5^2) + Kz_3 \\ \dot{z}_4 &= -f_2 z_4 - 0.5(z_2^2 - z_6^2) + Kz_4 \\ \dot{z}_5 &= -f_1 z_5 + z_1 z_7 - z_3 z_5 \\ \dot{z}_6 &= -f_1 z_6 + z_2 z_7 - z_4 z_6 \\ \dot{z}_7 &= -f_2 z_7 - z_1 z_5 + Kz_7 + 0.01z_1^2 + 2 + u_{ude} \end{aligned} \tag{25}$$

4.2. Simultaneous Synchronization and Anti-Synchronization Problem

In this part, the simultaneous synchronization and anti-synchronization of the laser system (15) are discussed, the study of which is mainly divided into two steps.

First, the nominal system was studied by using the method of dynamic gain feedback [20–22].

Theorem 2. System (15) has the following transformations, which can divide the system into two parts:

$$Z = \begin{pmatrix} Z_E \\ Z_e \end{pmatrix} = Nz \tag{26}$$

where matrix N is

$$N = \begin{pmatrix} 0 & 1 & 0 & 0 & 0 & 0 & 0 \\ 0 & 0 & 0 & 0 & 1 & 0 & 0 \\ 0 & 0 & 0 & 0 & 0 & 0 & 1 \\ 1 & 0 & 0 & 0 & 0 & 0 & 0 \\ 0 & 0 & 1 & 0 & 0 & 0 & 0 \\ 0 & 0 & 0 & 1 & 0 & 0 & 0 \\ 0 & 0 & 0 & 0 & 0 & 1 & 0 \end{pmatrix} \tag{27}$$

Under this transformation, chaotic system (15) can be transformed into the following two parts:

$$\dot{Z}_E = F_E(Z) = H(Z_e)Z_E \tag{28}$$

$$\dot{Z}_e = F_e(Z) = G(Z_E)Z_e \tag{29}$$

where $Z_E \in R^3, Z_e \in R^4$.

$$H(Z_e)Z_E = \begin{pmatrix} -f_1 + Z_{e4} & 0 & Z_{e6} \\ 0 & -f_1 - Z_{e3} & Z_{e1} \\ 0 & -Z_{e1} & -f_2 \end{pmatrix} \begin{pmatrix} Z_{E2} \\ Z_{E5} \\ Z_{E7} \end{pmatrix} \tag{30}$$

$$G(Z_E)Z_e = \begin{pmatrix} -f_1 & Z_{E2} & 0 & 0 \\ -0.5Z_{e1} & -f_2 & 0 & 0 \\ 0 & 0 & -f_2 & 0.5Z_{e6} \\ 0 & 0 & 0 & -f_1 - Z_{e4} \end{pmatrix} \begin{pmatrix} Z_{e1} \\ Z_{e3} \\ Z_{e4} \\ Z_{e6} \end{pmatrix} \tag{31}$$

This indicates that there is simultaneous synchronization and anti-synchronization problem in the system.

Proof of Theorem 2. The state of system (15) is z . Additionally, $F(z)$ is a continuous vector function. Let $\varphi = \text{diag}\{\varphi_1, \dots, \varphi_7\}$, where $|\varphi_m| = 1, m = 1, 2, \dots, 7$. Due to $F(\varphi z) = \varphi F(z)$, we can obtain the following equation and solution of z :

$$\begin{cases} (\varphi_1\varphi_3 - \varphi_1)z_1z_3 + (\varphi_5\varphi_7 - \varphi_1)z_5z_7 = 0 \\ (\varphi_2\varphi_4 - \varphi_2)z_2z_4 + (\varphi_6\varphi_7 - \varphi_2)z_6z_7 = 0 \\ (-\varphi_1^2 + \varphi_3)z_1^2 + (\varphi_5^2 - \varphi_3)z_5^2 = 0 \\ (-\varphi_2^2 + \varphi_4)z_2^2 + (\varphi_6^2 - \varphi_4)z_6^2 = 0 \\ (\varphi_1\varphi_7 - \varphi_5)z_1z_7 + (\varphi_5 - \varphi_3\varphi_5)z_3z_5 = 0 \\ (\varphi_2\varphi_7 - \varphi_6)z_2z_7 + (\varphi_6 - \varphi_4\varphi_6)z_4z_6 = 0 \\ (\varphi_7 - \varphi_1\varphi_5)z_1z_5 = 0 \end{cases} \tag{32}$$

$$\left\{ \begin{array}{l} \varphi_1 = \varphi_5 \varphi_7 \\ \varphi_2 = \varphi_6 \varphi_7 \\ \varphi_3 = 1 \\ \varphi_4 = 1 \\ \varphi_5 = \varphi_1 \varphi_7 \\ \varphi_6 = \varphi_2 \varphi_7 \\ \varphi_7 = \varphi_1 \varphi_5 \end{array} \right. \quad (33)$$

Make $\varphi_2 = -1$, and we can calculate a set of solutions as follows:

$$\rho^{(3)} = \begin{pmatrix} \varphi_2 \\ \varphi_5 \\ \varphi_7 \\ \varphi_1 \\ \varphi_3 \\ \varphi_4 \\ \varphi_6 \end{pmatrix} = \begin{pmatrix} -1 \\ -1 \\ -1 \\ 1 \\ 1 \\ 1 \\ 1 \end{pmatrix} \quad (34)$$

Thus, the N given in Equation (27) is obtained, which completes the proof. \square

According to this transformation, system (15) is divided into two systems. Make the main system as follows:

$$\dot{Z} = \begin{pmatrix} \dot{Z}_E \\ \dot{Z}_e \end{pmatrix} \quad (35)$$

where

$$\dot{Z}_E = F_E(Z) + b_1 u_c \quad (36)$$

$$\dot{Z}_e = F_e(Z) + b_2 u_c \quad (37)$$

where Z are the states; \dot{Z} , \dot{Z}_E , \dot{Z}_e are all derivatives; u_c is the controller.

$$b_1 = \begin{pmatrix} 0 \\ 0 \\ 1 \end{pmatrix}, b_2 = \begin{pmatrix} 0 \\ 1 \\ 0 \\ 0 \end{pmatrix} \quad (38)$$

Therefore, the corresponding slave system is

$$\dot{y} = \begin{pmatrix} \dot{y}_E \\ \dot{y}_e \end{pmatrix} \quad (39)$$

where

$$\dot{y}_E = F_E(y) \quad (40)$$

$$\dot{y}_e = F_e(y) \quad (41)$$

Let $E_E = Z_E + y_E$, and $E_e = y_e - Z_e$; then, the sum and error system can be expressed by the following Equation (42):

$$\dot{E} = S(Z, y, E) + b^* u_c \quad (42)$$

where

$$E = \begin{pmatrix} E_E \\ E_e \end{pmatrix}, b^* = \begin{pmatrix} b_1 \\ b_2 \end{pmatrix} \quad (43)$$

$$\begin{pmatrix} E_{E1} \\ E_{E2} \\ E_{E3} \\ E_{e1} \\ E_{e2} \\ E_{e3} \\ E_{e4} \end{pmatrix} = \begin{pmatrix} Z_{E2} + y_{E2} \\ Z_{E5} + y_{E5} \\ Z_{E7} + y_{E7} \\ y_{e1} - Z_{e1} \\ y_{e3} - Z_{e3} \\ y_{e4} - Z_{e4} \\ y_{e6} - Z_{e6} \end{pmatrix} \tag{44}$$

Theorem 3. The b_1 and b_2 are given in Equation (38); the designed controller is

$$u_c = kE \tag{45}$$

$$u_c = k(t) \begin{pmatrix} E_E \\ E_e \end{pmatrix} \begin{pmatrix} b_1 \\ b_2 \end{pmatrix}^T E = k(t) \begin{pmatrix} E_{E3} \\ E_{e2} \end{pmatrix} \tag{46}$$

$$\dot{k} = -\|E\|^2 \tag{47}$$

by which the sum and error system (40) is asymptotically stable. The master system (35) and the slave system (39) realize simultaneous synchronization and anti-synchronization.

Proof of Theorem 3. For the sum and error system (42), if $E_{E3} = E_{e2} = 0$, the subsystem $(\dot{E}_{E1} \ \dot{E}_{E2} \ \dot{E}_{e1} \ \dot{E}_{e3} \ \dot{E}_{e4})^T$ is asymptotically stable. Therefore, b^* is given in Equation (38), and it can be proved that $(S(Z, y, E), b^*)$ can be stabilized; therefore, the designed controller is reasonable [23,24]. \square

The controlled sum and error system is expressed as

$$\begin{aligned} \dot{E}_{E1} &= -f_1 E_{E1} + Z_{E2} Z_{e4} + Z_{e6} Z_{E7} + y_{E2} y_{e4} + y_{e6} y_{E7} \\ \dot{E}_{E2} &= -f_1 E_{E2} + Z_{E7} Z_{e1} - Z_{e3} Z_{E5} + y_{E7} y_{e1} - y_{e3} y_{E5} \\ \dot{E}_{E3} &= -f_2 E_{E3} - Z_{E5} Z_{e1} - y_{E5} y_{e1} + k(t) E_{E3} \\ \dot{E}_{e1} &= -f_1 E_{e1} + y_{e1} y_{e3} + y_{E5} y_{E7} - Z_{e1} Z_{e3} - Z_{E5} Z_{E7} \\ \dot{E}_{e2} &= -f_2 E_{e2} + 0.5(Z_{e1}^2 - Z_{E5}^2 - y_{e1}^2 + y_{E5}^2) + k(t) E_{e2} \\ \dot{E}_{e3} &= -f_2 E_{e3} + 0.5(Z_{E2}^2 - Z_{e6}^2 - y_{E2}^2 + y_{e6}^2) \\ \dot{E}_{e4} &= -f_1 E_{e4} - y_{e4} y_{e6} + y_{E2} y_{E7} + Z_{e4} Z_{e6} - Z_{E2} Z_{E7} \end{aligned} \tag{48}$$

Second, let the main system be as follows:

$$\dot{Z} = F(Z) + b^* u_c + \Delta f(Z) + d(Z) + b^* u_{ude1} \tag{49}$$

where $F(Z) = \begin{pmatrix} F_E(Z) \\ F_e(Z) \end{pmatrix}$, $b^* = \begin{pmatrix} b_1 \\ b_2 \end{pmatrix}$, $b_1 = \begin{pmatrix} 0 \\ 0 \\ 1 \end{pmatrix}$, and u_c is given in Equation (46),

$d(Z) \in R^7$ is the external disturbance to the system, $\Delta f(Z)$ is the uncertainty of the

system, the initial condition is set to $\Delta f(Z) = \begin{pmatrix} 0 \\ 0 \\ 0.01Z_{E1} \\ 0 \\ 0.01Z_{E1} \\ 0 \\ 0 \end{pmatrix}$, $d(Z) = \begin{pmatrix} 0 \\ 0 \\ 1 \\ 0 \\ 1 \\ 0 \\ 0 \end{pmatrix}$ in this paper

(the external perturbations and uncertainties are only randomly selected values, and for

convenience, in this paper, $z_1 = z_2 = z_4 = z_6 = z_7 = 0$). u_{ude1} is the controller to be designed. Additionally, the slave system is

$$\dot{y} = F(y) \tag{50}$$

where $F(y) = \begin{pmatrix} F_E(y) \\ F_e(y) \end{pmatrix}$; let $E_E = Z_E + y_E$, and $E_e = y_e - Z_e$; then, the sum and error system is

$$\dot{E} = F(E) + b^* u_c + \Delta f(Z) + d(Z) + b^* u_{ude1} \tag{51}$$

According to Lemma 2, u_{ude1} can be obtained, and the filter selection is

$$G(s) = \frac{1}{1 + 0.001s} \tag{52}$$

$$\begin{aligned} \dot{E}_{E1} &= -f_1 E_{E1} + Z_{E2} Z_{e4} + Z_{e6} Z_{E7} + y_{E2} y_{e4} + y_{e6} y_{E7} \\ \dot{E}_{E2} &= -f_1 E_{E2} + Z_{E7} Z_{e1} - Z_{e3} Z_{E5} + y_{E7} y_{e1} - y_{e3} y_{E5} \\ \dot{E}_{E3} &= -f_2 E_{E3} - Z_{E5} Z_{e1} - y_{E5} y_{e1} + k(t) E_{E3} + \Delta f(Z) + d(Z) + u_{ude1} \\ \dot{E}_{e1} &= -f_1 E_{e1} + y_{e1} y_{e3} + y_{E5} y_{E7} - Z_{e1} Z_{e3} - Z_{E5} Z_{E7} \\ \dot{E}_{e2} &= -f_2 E_{e2} + 0.5(Z_{e1}^2 - Z_{E5}^2 - y_{e1}^2 + y_{E5}^2) + k(t) E_{e2} + \Delta f(Z) + d(Z) + u_{ude1} \\ \dot{E}_{e3} &= -f_2 E_{e3} + 0.5(Z_{E2}^2 - Z_{e6}^2 - y_{E2}^2 + y_{e6}^2) \\ \dot{E}_{e4} &= -f_1 E_{e4} - y_{e4} y_{e6} + y_{E2} y_{E7} + Z_{e4} Z_{e6} - Z_{E2} Z_{E7} \end{aligned} \tag{53}$$

5. Results

5.1. Simulation of Stabilization

The following results can be obtained by using MATLAB simulation. Let the initial value $z(0) = (1 \ 1 \ 2 \ 2 \ 3 \ 3 \ 2)$, and the feedback gain $K(0) = -1$. Firstly, for the nominal system (13), the seven states of the system are gradually stable from Figure 2. Figure 3 shows the dynamic gain feedback eventually becomes an appropriate constant. This shows u_a in (17) is reasonable. Each state of the system (14) finally approaches zero, and the stabilization of the system is realized.

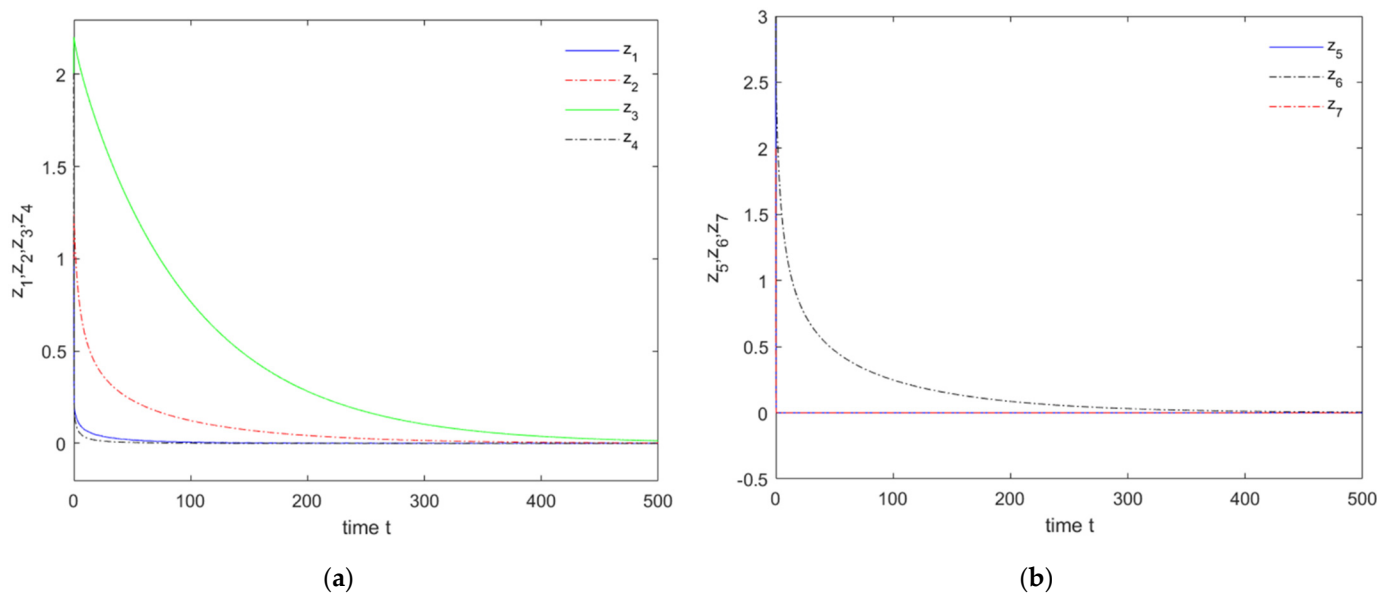


Figure 2. The state diagram of system: (a) the state diagram of z_1, z_2, z_3, z_4 ; (b) the state diagram of z_5, z_6, z_7 .

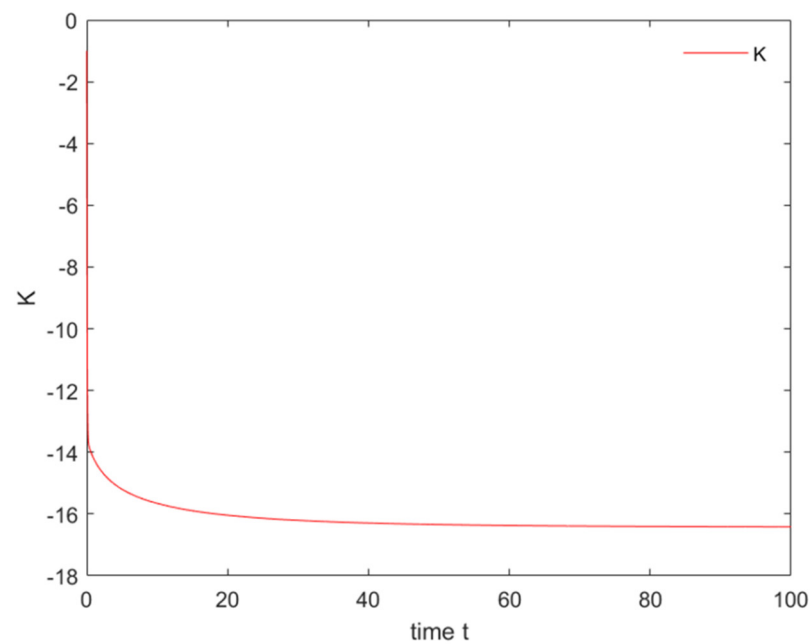


Figure 3. The state diagram of dynamic feedback gain K .

Next, the initial value above was selected, and system (4) was simulated. As evident from Figure 4, the states of the system are gradually stable. Figure 5 reveals that the dynamic gain gradually becomes constant, and Figure 6 shows the two lines gradually coincide, indicating that u_d tends to be equal to its estimated value of \hat{u}_d . In the case of external disturbance, the system is stabilized under the action of the controller.

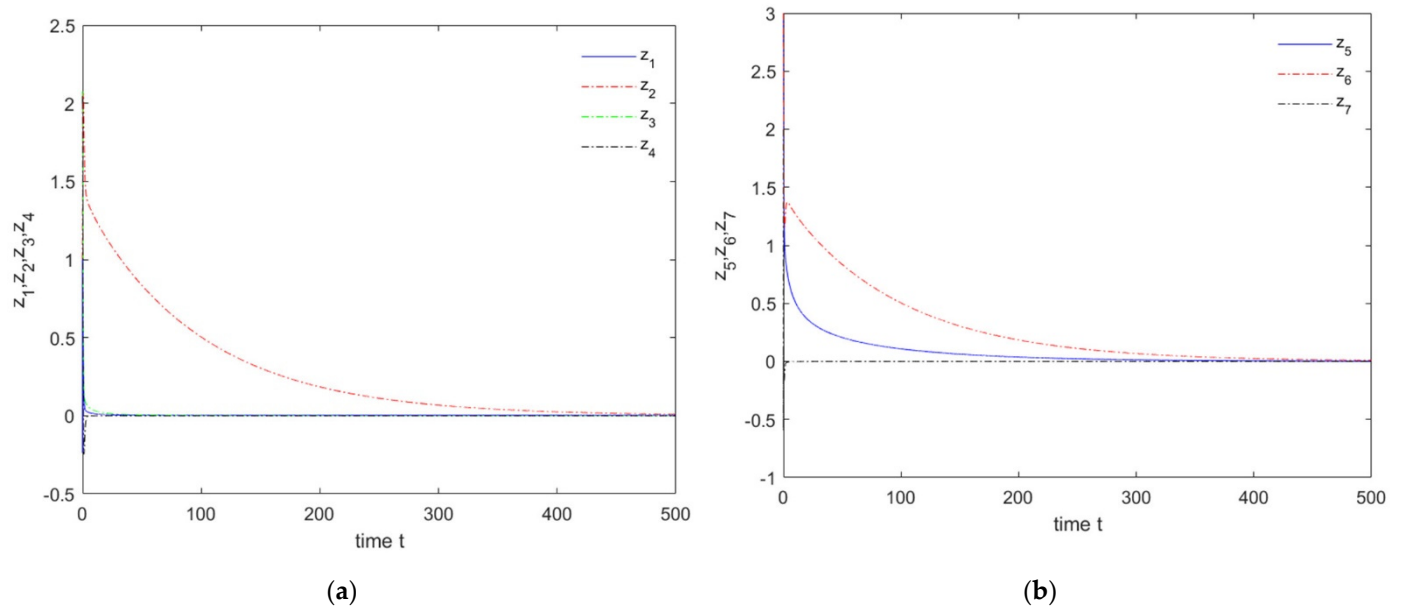


Figure 4. The state diagram of system based on UDE control method: (a) the state diagram of z_1, z_2, z_3, z_4 ; (b) the state diagram of z_5, z_6, z_7 .

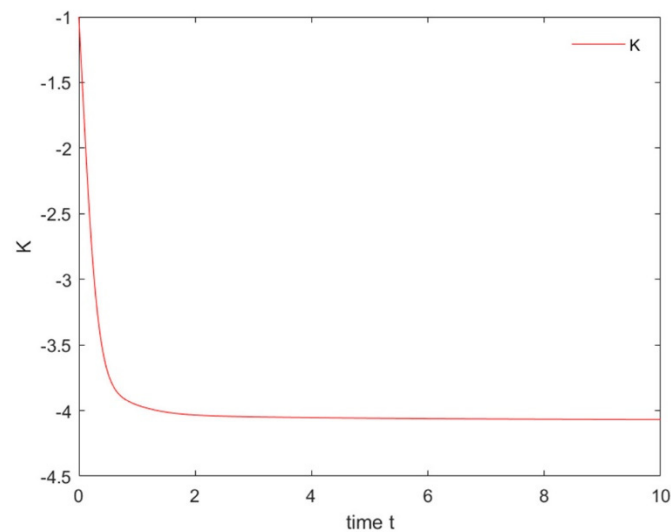


Figure 5. The state diagram of feedback gain K .

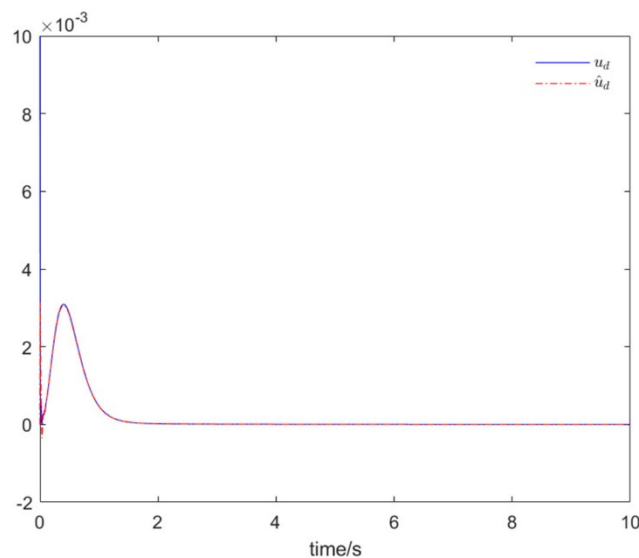


Figure 6. u_d gradually approaches the same as \hat{u}_d .

5.2. Simulation of Simultaneous Synchronization and Anti-Synchronization

The following results can be obtained by using MATLAB simulation:

Firstly, simulation was used to verify the correctness of the dynamic gain control method. Let the initial values are $Z_E(0) = (0.2, 0.2, 0.1)$, $y_{E1} = y_{E2} = y_{E3} = 0.2$, $Z_e(0) = (0.1, 0.2, 0.3, 0.1)$, and $y_e(0) = (0.2, 0.3, 0.2, 0.1)$. Additionally, the feedback gain is $k(0) = -1$.

Figure 7 shows the feedback gain k gradually approaches a constant. Figure 8a,b show the states of the sum system E_E and error system E_e , respectively. We can see that they all tend to stabilize in the end. The states Z_E and the corresponding states y_E are anti-synchronous, as evident from Figure 9. Figure 10 reveals that the states Z_e and the corresponding states y_e are synchronized.

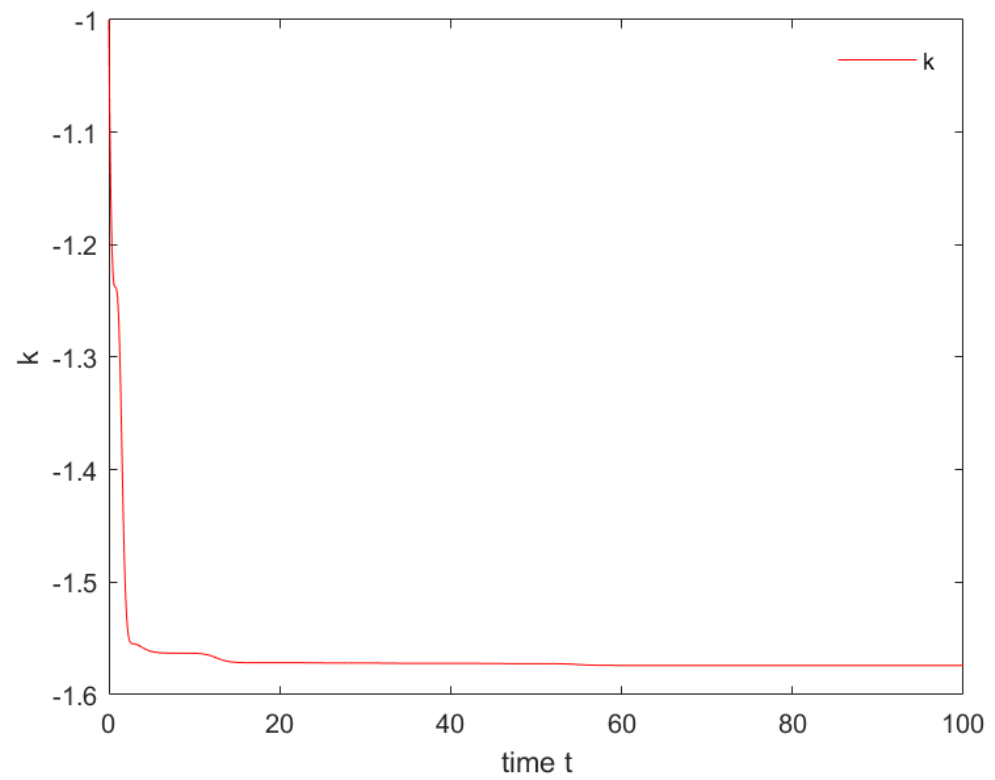
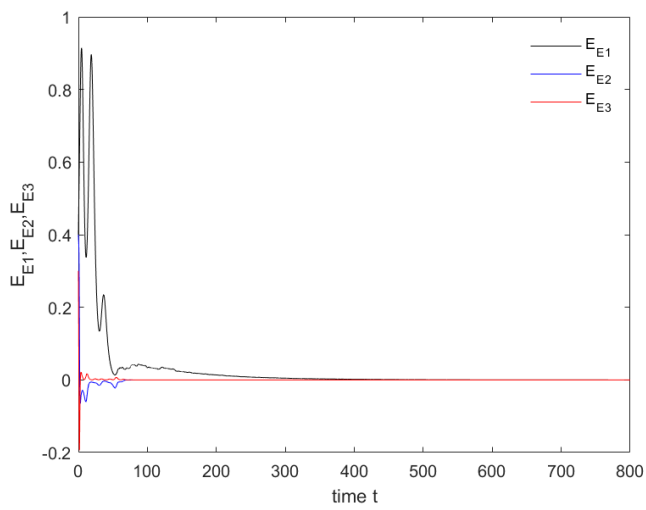
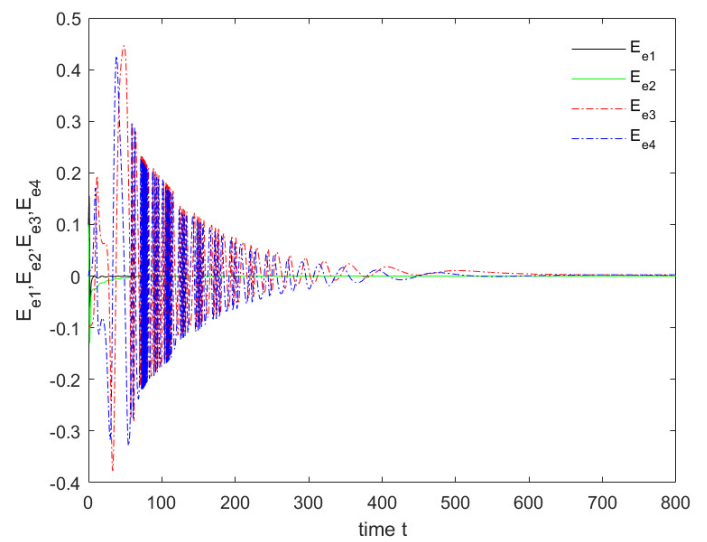


Figure 7. The state diagram of dynamic feedback gain k .



(a)



(b)

Figure 8. The state diagram of system: (a) the state diagram of sum system; (b) the state diagram of error system.

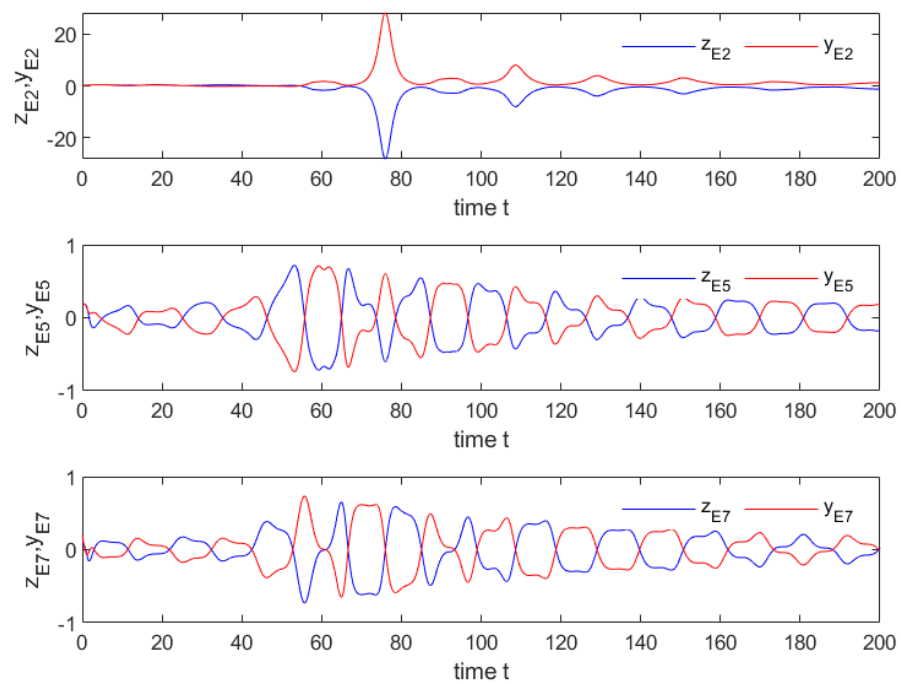


Figure 9. The state diagram of Z_E, y_E . The state diagram under dynamic gain feedback control method.

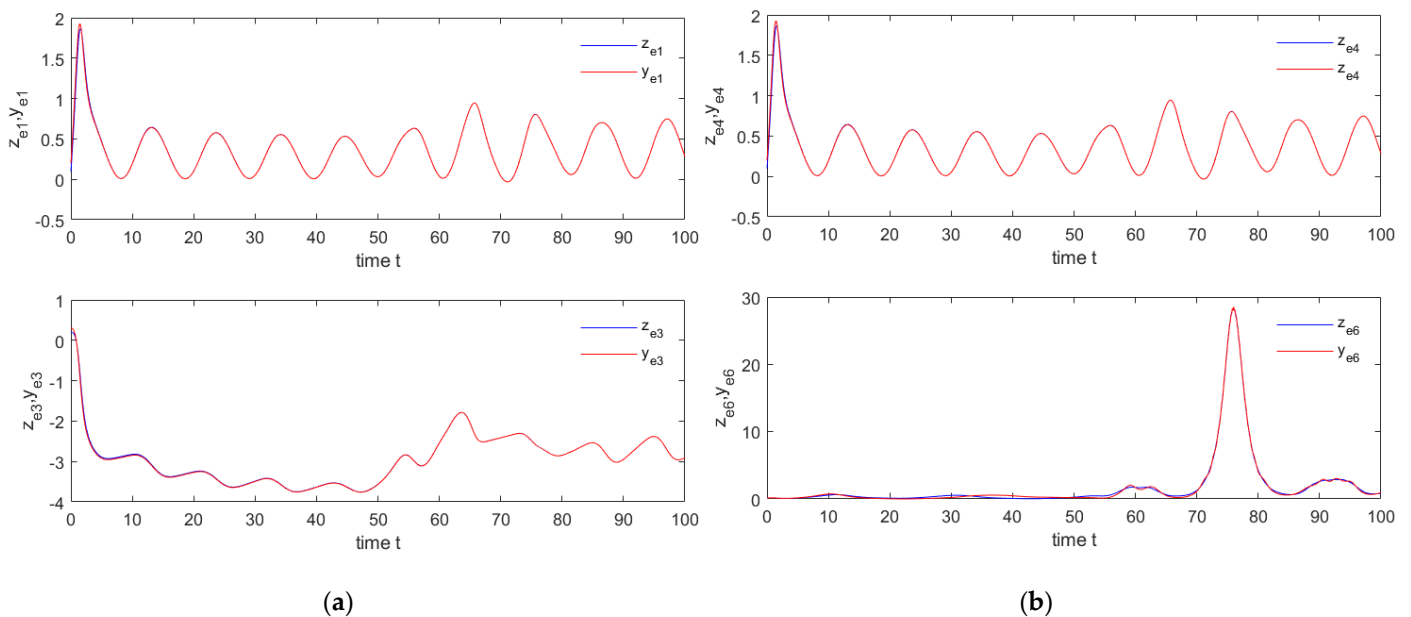


Figure 10. The state diagram of Z_e, y_e : (a) Z_{e1}, y_{e1} and Z_{e3}, y_{e3} are synchronized, respectively; (b) Z_{e4}, y_{e4} and Z_{e6}, y_{e6} are synchronized, respectively.

Next, the system with uncertainty and disturbance was simulated. The above initial value was selected, and the following results can be obtained:

Figure 11 shows the states of the sum and error system gradually approaching zero. Figure 12 shows three states in the system that realize anti-synchronization, while Figure 13 shows the other four states in the system realize synchronization.

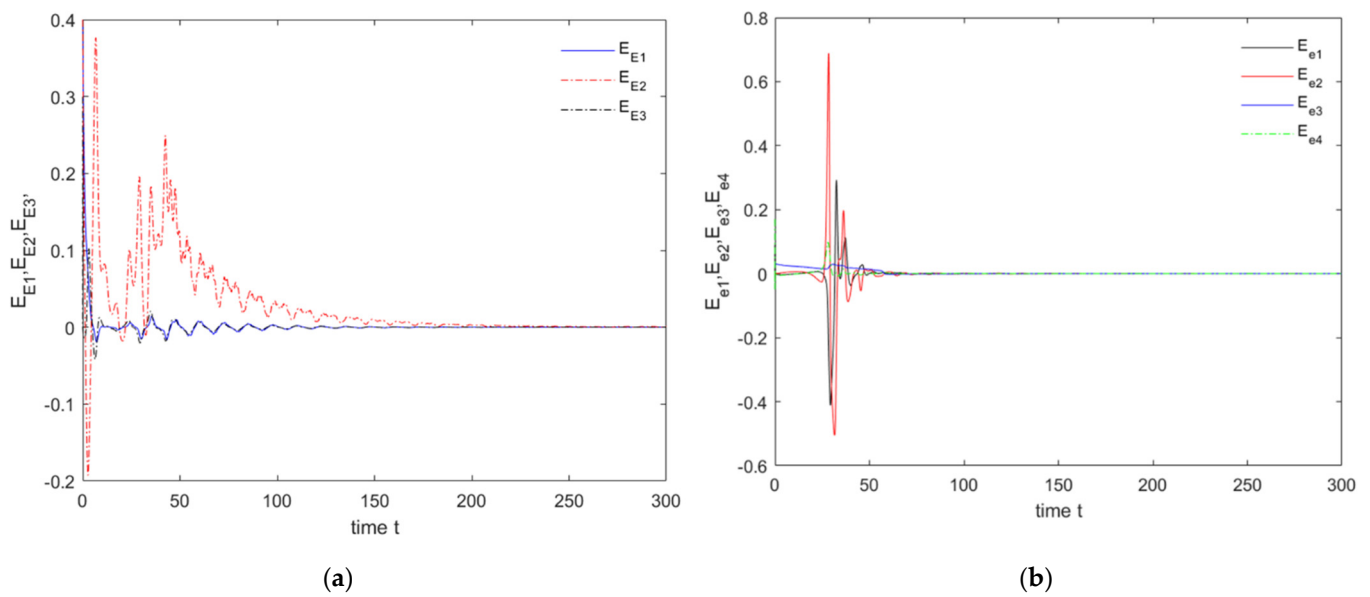


Figure 11. The state diagram of E_E, E_e : (a) the state diagram of E_E ; (b) the state diagram of E_e .

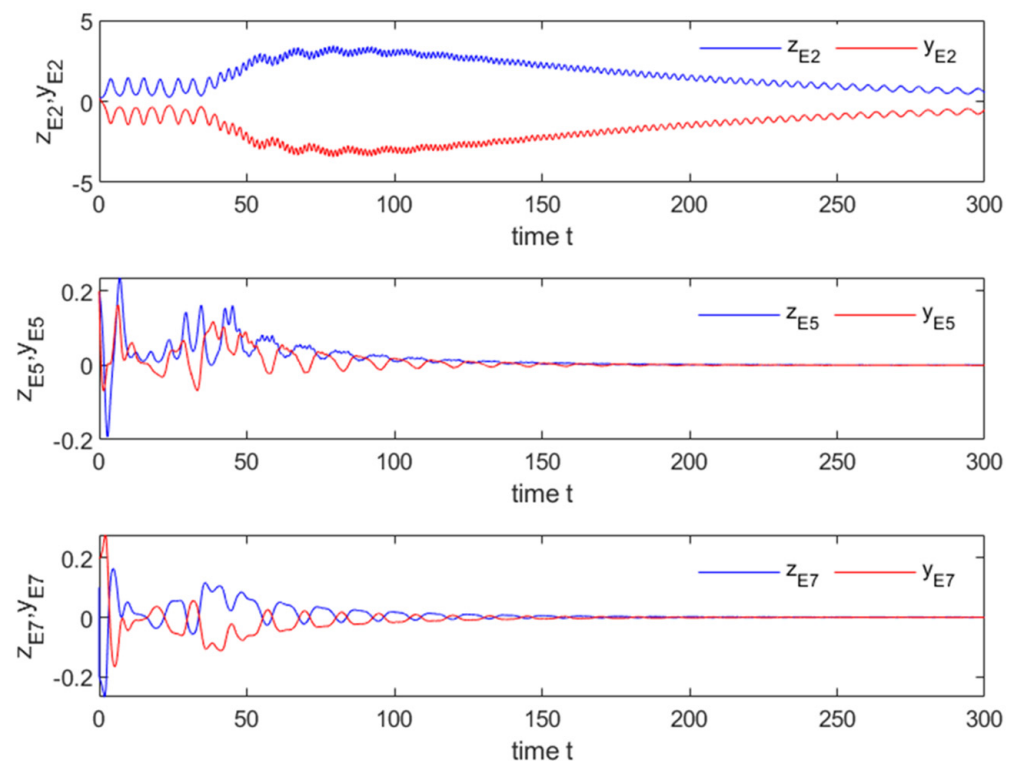


Figure 12. The state diagram of Z_E, y_E . The state diagram based on UDE dynamic control method.

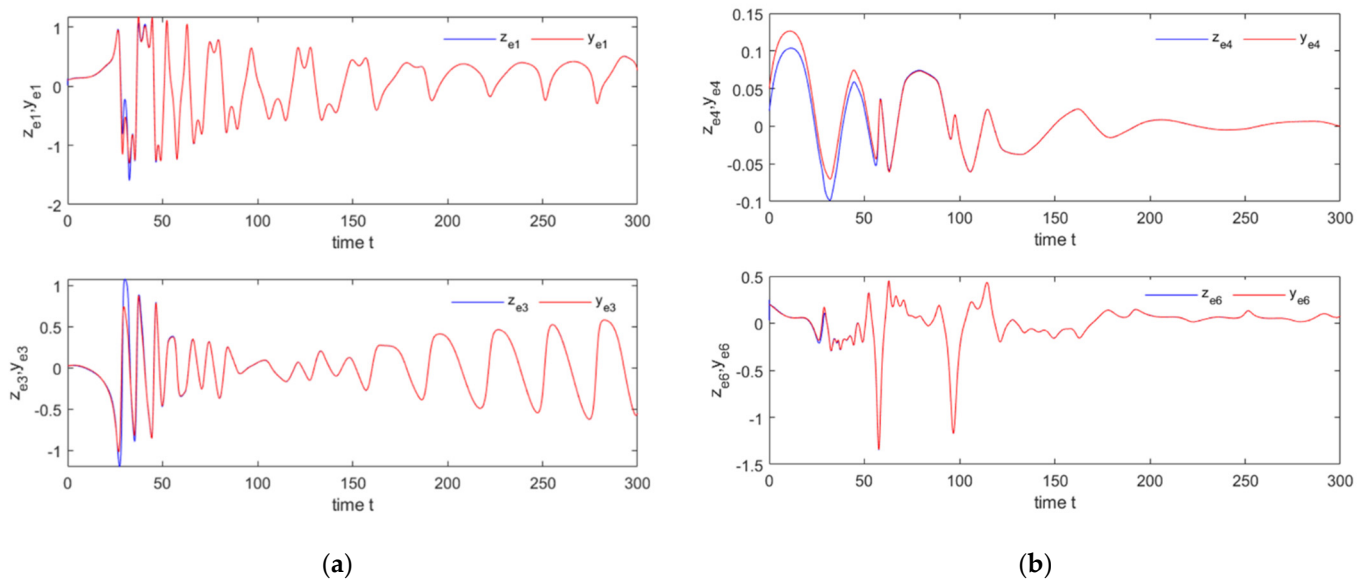


Figure 13. The state diagram of Z_e, y_e : (a) the state diagram of $Z_{e1}, y_{e1}, Z_{e3}, y_{e3}$; (b) the state diagram of $Z_{e4}, y_{e4}, Z_{e6}, y_{e6}$.

Figure 14 reflects that the uncertainties and disturbances u_{d1} and u_{d2} of the system tend to be the same as their estimated values \hat{u}_{d1} and \hat{u}_{d2} , respectively. Figure 15 indicates that the feedback gain gradually converges to a constant.

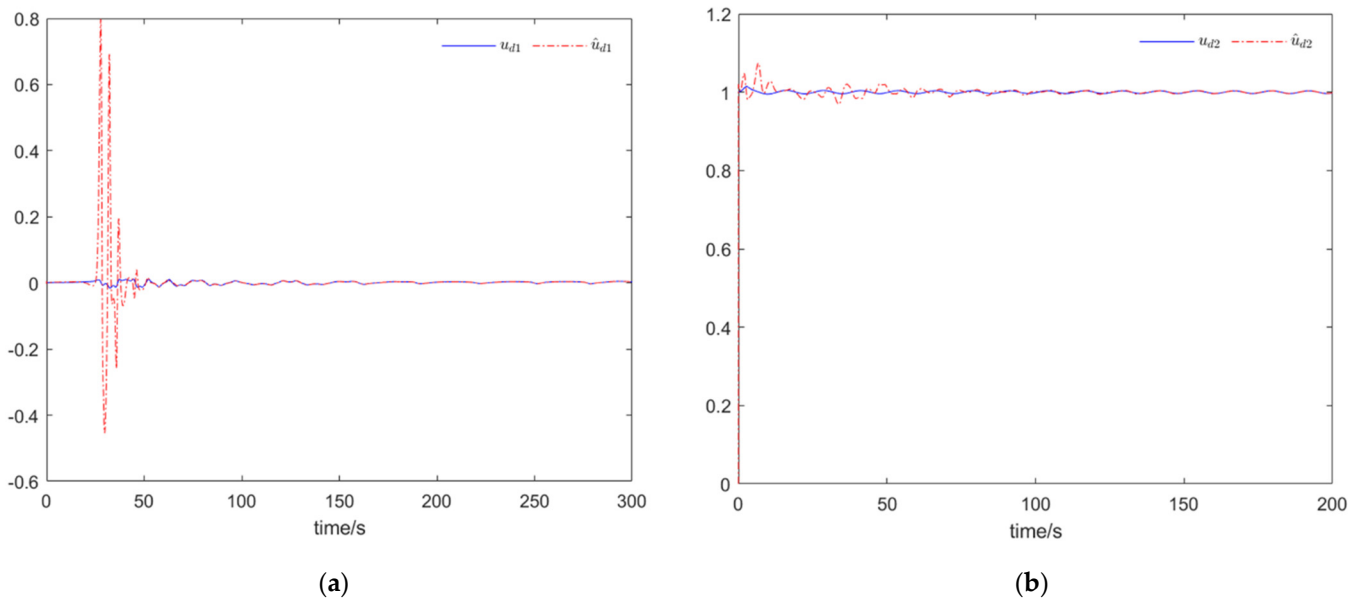


Figure 14. The state diagram of uncertainty and disturbance: (a) u_{d1} gradually approaches the same as \hat{u}_{d1} ; (b) u_{d2} gradually approaches the same as \hat{u}_{d2} .

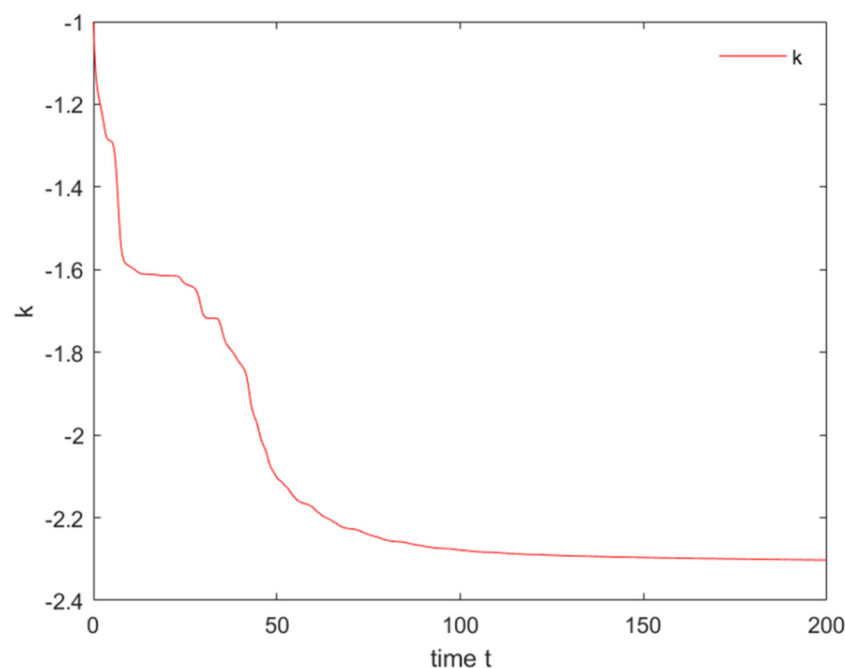


Figure 15. The feedback gain k finally approaches a constant.

5.3. Discussion

When using the dynamic gain feedback control method, it took about 400 s for E_E to realize anti-synchronization and 700 s for E_e to realize synchronization. When the second method was adopted, it took about 250 s for E_E to realize anti-synchronization, and E_e realized synchronization in less than 100 s. The proposed system can realize simultaneous synchronization and anti-synchronization faster. At the same time, we can see that when the second method was adopted, the state change range of the laser system is relatively small and more stable. Through the simulation comparison of the two methods, the dynamic feedback method based on UDE can realize the stability of the system in the environment with external disturbances, and the feedback gain can be changed flexibly.

The results show that this new chaotic system is worth studying because of its obvious chaotic characteristics. It is better to use the UDE control method combined with dynamic feedback gain. The form of the controller designed using this method is relatively simple, and it is possible to determine whether the system achieves synchronization and anti-synchronization by monitoring the data and state of the feedback gain during operation. Additionally, it can eliminate the uncertainty and interference of the system. This method can be used in most nonlinear system control fields. Although this method is superior to the dynamic feedback control method, it has some limitations. The cut-off frequency of the filter determines the sum of uncertainty and interference.

Due to the randomness and ergodicity of chaos [23–28], chaos has important research value in the field of random coverage path planning of chaotic mobile robots. The control problem of laser systems studied in this paper provides a new idea for research on chaotic robots. The designed controllers are physically realizable, which provides a theoretical basis for the synchronization and stabilization of chaotic robots in the future.

6. Conclusions

In this paper, the stabilization and synchronization of a chaotic system in a complex domain were studied by using the control method of dynamic gain feedback, and the appropriate controllers were designed. Then, combining this method with the UDE control method, the controllers suitable for laser complex chaotic systems with external interference and uncertainty were designed. Therefore, the stabilization, simultaneous synchronization, and partial anti-synchronization of the system were realized. The simulation results show

that this method is effective and has more advantages. The dynamic feedback control method based on UDE can change the feedback gain and obtain a more flexible controller, as well as solve the problem that the system can still achieve synchronization and partial anti-synchronization under uncertain interference, and reduce the asymmetry of nonlinear system. The research results provide a theoretical basis for the application of chaotic mobile robots in complex chaotic systems.

Author Contributions: Writing—review and editing, Z.W.; data curation, writing—original draft preparation, Z.W. and J.P. Review, L.M. and G.W. All authors have read and agreed to the published version of the manuscript.

Funding: This research was funded by the National Natural Science Foundation of China (61903207).

Institutional Review Board Statement: Not applicable.

Informed Consent Statement: Not applicable.

Data Availability Statement: All data, models, and codes generated or used during the study appear in the submitted article.

Conflicts of Interest: The authors declare no conflict of interest.

References

1. Vishal, K.; Agrawal, S.K. On dynamics, existence of chaos, control and synchronization of novel complex chaotic system. *Chin. J. Phys.* **2017**, *55*, 519–532. [[CrossRef](#)]
2. Guo, R. A simple adaptive controller for chaos and hyperchaos synchronization. *Phys. Lett. A* **2008**, *372*, 5593–5597. [[CrossRef](#)]
3. Zhu, Z.Y.; Zhao, Z.S.; Zhang, J.; Wang, R.K.; Li, Z. Adaptive fuzzy control design for synchronization of chaotic time-delay system. *Inf. Sci.* **2020**, *535*, 17. [[CrossRef](#)]
4. Sugitani, Y.; Zhang, Y.; Motter, A.E. Synchronizing Chaos with Imperfections. *Phys. Rev. Lett.* **2021**, *126*, 164101. [[CrossRef](#)]
5. Fan, L.; Yan, X.; Wang, H.; Wang, L.V. Real-time observation and control of optical chaos. *Sci. Adv.* **2021**, *7*, eabc8448. [[CrossRef](#)] [[PubMed](#)]
6. Liu, Y.Z.; Xie, Y.Y.; Ye, Y.C.; Zhang, J.P.; Wang, S.J.; Liu, Y.; Pan, G.F.; Zhang, J.L. Exploiting Optical Chaos With Time-Delay Signature Suppression for Long-Distance Secure Communication. *IEEE Photonics J.* **2017**, *9*, 12. [[CrossRef](#)]
7. Heidarzadeh, S.; Shahmoradi, S.; Shahrokhi, M. Adaptive synchronization of two different uncertain chaotic systems with unknown dead-zone input nonlinearities. *J. Vib. Control* **2020**, *26*, 1956–1968. [[CrossRef](#)]
8. Yuan, G.H.; Zhang, X.; Wang, Z.R. Generation and synchronization of feedback-induced chaos in semiconductor ring lasers by injection-locking. *Optik* **2014**, *125*, 1950–1953. [[CrossRef](#)]
9. Mahmoud, E.; Al-Harhi, B. A hyperchaotic detuned laser model with an infinite number of equilibria existing on a plane and its modified complex phase synchronization with time lag. *Chaos Solitons Fractals* **2020**, *130*, 109442. [[CrossRef](#)]
10. Kashyap Anisha, R.V.; Kolwankar Kiran, M. Hyperchaos and synchronization in two element nonlinear chimney model. *Chaos* **2020**, *30*, 123114. [[CrossRef](#)]
11. Nakamura, Y.; Sekiguchi, A. The chaotic mobile robot. *IEEE Trans. Robot. Autom.* **2001**, *17*, 898–904. [[CrossRef](#)]
12. Martins-Filho, L.S.; Macau, E.E.N. Patrol Mobile Robots and Chaotic Trajectories. *Math. Probl. Eng.* **2014**, *2007*, 57–76. [[CrossRef](#)]
13. Li, C.H.; Song, Y.; Wang, F.Y.; Wang, Z.Q.; Li, Y.B. A Chaotic Coverage Path Planner for the Mobile Robot, Based on the Chebyshev Map for Special Missions. *Front. Inf. Technol. Electron. Eng.* **2017**, *18*, 1305–1319. [[CrossRef](#)]
14. Qiu, C.; Xiao, J.; Yu, L.; Han, L.; Iqbal, M.N. A Modified Interval Type-fuzzy Cmeans Algorithm with Application in MR Image Segmentation. *Pattern Recognit. Lett.* **2013**, *34*, 1329–1338. [[CrossRef](#)]
15. Ren, L.; Guo, R.; Vincent, U.E. Coexistence of synchronization and anti-synchronization in chaotic systems. *Arch. Control Sci.* **2016**, *26*, 69–79. [[CrossRef](#)]
16. Peng, R.; Jiang, C.; Guo, R. Partial Anti-Synchronization of the Fractional-Order Chaotic Systems through Dynamic Feedback Control. *Mathematics* **2021**, *9*, 718. [[CrossRef](#)]
17. Guo, R. Projective synchronization of a class of chaotic systems by dynamic feedback control method. *Nonlinear Dyn.* **2017**, *90*, 53–64. [[CrossRef](#)]
18. Guo, R.; Zhang, Y.; Jiang, C. Synchronization of Fractional-Order Chaotic Systems with Model Uncertainty and External Disturbance. *Mathematics* **2021**, *9*, 877. [[CrossRef](#)]
19. Fang, J.; Jiang, M.; An, X.; Deng, W. Construction of laser complex chaotic system and synchronization of dot product Function projection. *Complex Syst. Complex. Sci.* **2021**, *18*, 30–37. (In Chinese)
20. Buscarino, A.; Fortuna, L.; Patané, L. Master-slave synchronization of hyperchaotic systems through a linear dynamic coupling. *Phys. Rev.* **2019**, *100*, 032215. [[CrossRef](#)] [[PubMed](#)]
21. E Mahmoud, E.; A Al-Adwani, M. Complex anti-synchronization of two indistinguishable chaotic complex nonlinear models. *Meas. Control* **2019**, *52*, 922–928. [[CrossRef](#)]

22. Meng, F.; Zeng, X.; Wang, Z. Impulsive anti-synchronization control for fractional-order chaotic circuit with memristor. *Indian J. Phys.* **2019**, *93*, 1187–1194. [[CrossRef](#)]
23. Ren, B.; Zhong, Q.-C.; Dai, J. Asymptotic Reference Tracking and Disturbance Rejection of UDE-Based Robust Control. *IEEE Trans. Ind. Electron.* **2016**, *64*, 3166–3176. [[CrossRef](#)]
24. Matsumoto, T. A Chaotic Attractor from Chua's Circuit. *IEEE Trans. Circuits Syst.* **1985**, *31*, 1055–1058. [[CrossRef](#)]
25. Dong, Y.; Ren, B. UDE-Based Variable Impedance Control of Uncertain Robot Systems. *IEEE Trans. Syst. Man Cybern. Syst.* **2017**, *49*, 2487–2498. [[CrossRef](#)]
26. Khennaoui, A.-A.; Ouannas, A.; Bendoukha, S.; Grassi, G.; Wang, X.; Pham, V.-T.; Alsaadi, F.E. Chaos, control, and synchronization in some fractional-order difference equations. *Adv. Differ. Equ.* **2019**, *2019*, 412. [[CrossRef](#)]
27. Guo, R.-W. Simultaneous Synchronization and Anti-Synchronization of Two Identical New 4D Chaotic Systems. *Chin. Phys. Lett.* **2011**, *28*, 040205. [[CrossRef](#)]
28. Postnov, D.E.; Shishkin, A.V.; Sosnovtseva, O.V.; Mosekilde, E. Two-mode chaos and its synchronization properties. *Phys. Rev. E* **2005**, *72*, 056208. [[CrossRef](#)]